Naval Research Laboratory
Washington, DC 20375-5320

NRL/7260/MR—2023/1

Estimation of Breaking Wave Height from Ultrawideband Radar Data

DR. MARK A. SLETTEN

Radar Sensing and Analysis Section
Remote Sensing Division

September 29, 2023

REPORT DOCUMENTATION PAGE

Form Approved
OMB No. 0704-0188

1. REPORT DATE *(DD-MM-YYYY)*	**2. REPORT TYPE**	**3. DATES COVERED** *(From - To)*
28-09-2023	NRL Memorandum Report	

4. TITLE AND SUBTITLE

Estimation of Breaking Wave Height from Ultrawideband Radar Data

5a. CONTRACT NUMBER

5b. GRANT NUMBER

5c. PROGRAM ELEMENT NUMBER

6. AUTHOR(S)

Dr. Mark Sletten

5d. PROJECT NUMBER

5e. TASK NUMBER

5f. WORK UNIT NUMBER
6D45

7. PERFORMING ORGANIZATION NAME(S) AND ADDRESS(ES)

Naval Research Laboratory
4555 Overlook Avenue, SW
Washington, DC 20375-5320

8. PERFORMING ORGANIZATION REPORT NUMBER

NRL/7260/MR--2023/1

9. SPONSORING / MONITORING AGENCY NAME(S) AND ADDRESS(ES)

Office of Naval Research
One Liberty Center
875 N Randolph Street
Arlington, VA 22217-1995

10. SPONSOR / MONITOR'S ACRONYM(S)

11. SPONSOR / MONITOR'S REPORT NUMBER(S)

12. DISTRIBUTION / AVAILABILITY STATEMENT

DISTRIBUTION STATEMENT A: Approved for public release; distribution is unlimited.

13. SUPPLEMENTARY NOTES

14. ABSTRACT

In this report, we describe a multipath model for the microwave backscatter produced by breaking water waves that promises to provide a means to estimate breaker height when applied to ultrawideband (UWB) radar data. Particularly at low grazing angles, multipath scattering between the wave crest and the front face of the breaker is known to play an important role in the scattering mechanism. From a ray tracing perspective, the scattering can follow a direct path from the radar to the crest and back again, or its path can involve a bounce off the front face. Interference between components that follow these different paths produces peaks and nulls when the backscatter data is viewed in the RF frequency domain, with the peak spacing dependent upon the grazing angle and the breaker height. The simple model described in this report provides the analysis required to estimate the breaker height from the location of the peaks. The model indicates that very low grazing angles less than 5° are preferable, as the peak spacing is then wide enough to measure with modest frequency resolution while the distinctive polarization response of the front-face reflection coefficient also provides a means to reject signals that are not generated by the assumed multipath mechanism.

15. SUBJECT TERMS

Ultrawideband radar
Breaking ocean waves

16. SECURITY CLASSIFICATION OF:			**17. LIMITATION OF ABSTRACT**	**18. NUMBER OF PAGES**	**19a. NAME OF RESPONSIBLE PERSON**
					Dr. Mark Sletten
a. REPORT	**b. ABSTRACT**	**c. THIS PAGE**	U	14	**19b. TELEPHONE NUMBER** *(include area code)*
U	U	U			(202) 404-7971

Standard Form 298 (Rev. 8-98)
Prescribed by ANSI Std. Z39.18

This page intentionally left blank.

Executive Summary

In this report, we describe a multipath model for the microwave backscatter produced by breaking water waves that promises to provide a means to estimate breaker height when applied to ultrawideband (UWB) radar data. Particularly at low grazing angles, multipath scattering between the wave crest and the front face of the breaker is known to play an important role in the scattering mechanism. From a ray tracing perspective, the scattering can follow a direct path from the radar to the crest and back again, or its path can involve a bounce off the front face. Interference between components that follow these different paths produces peaks and nulls when the backscatter data is viewed in the RF frequency domain, with the peak spacing dependent upon the grazing angle and the breaker height. The simple model described in this report provides the analysis required to estimate the breaker height from the location of the peaks. The model indicates that very low grazing angles less than 5° are preferable, as the peak spacing is then wide enough to measure with modest frequency resolution while the distinctive polarization response of the front-face reflection coefficient also provides a means to reject signals that are not generated by the assumed multipath mechanism.

This page intentionally left blank.

Introduction

Radar backscatter from breaking water waves has been studied for nearly four decades [1-5, 7-13, 15-25]. Motivation for this research stems from the fact that the backscatter can be target-like, thereby posing a significant false alarm challenge for target detection algorithms, and because radar-based remote sensing of breaking waves can provide a means to estimate important environmental and geophysical parameters, including air-sea interactions and bathymetry. This research provides strong evidence that multipath interference plays an important role in the scattering mechanism when the grazing angle is low, that is, when the radar views the breaker at an angle nearly parallel to the mean water surface [13-16, 19-23].

In particular, our research in [16] presents a preliminary analysis of UWB radar data collected in the field that uses the apparent multipath interference patterns to provide an estimate of the breaker height. Given the importance of wave height measurement, particularly in the surf zone, in this report we further develop the multipath model underlying this analysis. This model is then used to predict the basic characteristics of the backscatter and provide guidance on the selection of grazing angle and polarization.

Model Description

A sketch illustrating the model is shown in Figure 1. The breaker has a crest height h, and the radar grazing angle is ψ. A small breaking plume located near the crest is assumed to be the primary scattering center. In the spirit of ray optics, four components to the total backscatter are involved: 1) a "direct-direct" (dd) component that follows a direct path from the radar to the plume and back, 2) a "direct-

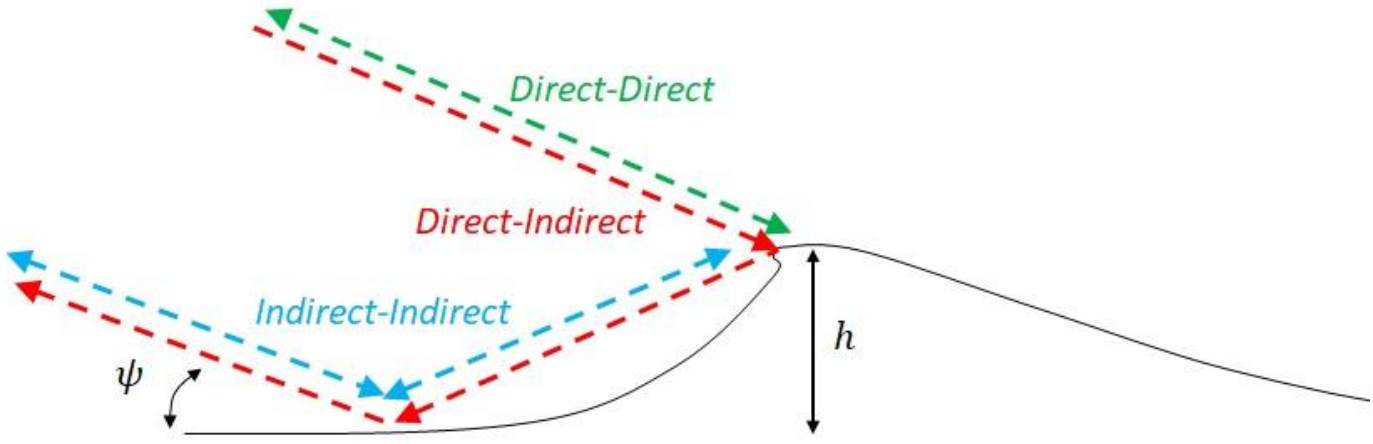

Figure 1. Sketch of the model showing the components of the multipath backscatter

Manuscript approved September 27, 2023.

indirect" (*di*) component that follows a path back to the radar that involves a reflection off the front face, 3) an "indirect-direct' (*id*) component that follows a path identical to the *di* path except in the reverse direction (for clarity, not shown in Fig 1), and 4) an "indirect-indirect" (*ii*) component that experiences a bounce off the front face both before and after scattering off the plume. From simple geometry, the difference between the *dd* and *di* propagation path lengths can be computed to be

$$\Delta = 2h\sin(\psi) \qquad (1)$$

while the difference between the *dd* and *ii* paths is 2Δ. The total backscatter is the coherent sum of all four components, which can be expressed as

$$s^{VV} = r_{dd}^{VV} + 2\rho^{VV}\exp(ik\Delta)\, r_{di}^{VV} + (\rho^{VV})^2\exp(i2k\Delta)\, r_{ii}^{VV} \qquad (2)$$

$$s^{HH} = r_{dd}^{HH} + 2\rho^{HH}\exp(ik\Delta)\, r_{di}^{HH} + (\rho^{HH})^2\exp(i2k\Delta)\, r_{ii}^{HH} \qquad (3)$$

where $= 2\pi/\lambda$, λ is the radar wavelength, and the VV and HH superscripts refer to vertical and horizontal polarization, respectively. The factors of the form r_{pq}^{PP} represent the complex scattering coefficients of the plume for each of the ray path (pq) and polarization (PP) combinations. ρ^{PP} is the complex reflection coefficient describing the "bounce" off the front face experienced by the *di*, *id*, and *ii* components and can be computed using expressions found in textbooks that discuss oblique electromagnetic reflections at the interface between two dielectrics. In this work, we use the following equations taken from [14] to compute ρ^{PP}:

$$\rho^{VV} = \frac{Z_L^{VV} - Z_{z1}^{VV}}{Z_L^{VV} + Z_{z1}^{VV}} \qquad \rho^{HH} = \frac{Z_L^{HH} - Z_{z1}^{HH}}{Z_L^{HH} + Z_{z1}^{HH}} \qquad (4)$$

$$Z_L^{VV} = \eta_2\sqrt{1 - \frac{\epsilon_1}{\epsilon_2}\cos(\psi)^2} \qquad Z_L^{HH} = \frac{\eta_2}{\sqrt{1 - \frac{\epsilon_1}{\epsilon_2}\cos(\psi)^2}} \qquad (5)$$

$$Z_{z1}^{VV} = \eta_1\sin(\psi) \qquad Z_{z1}^{HH} = \frac{\eta_1}{\sin(\psi)} \qquad (6)$$

$$\eta_1 = \sqrt{\frac{\mu_0}{\epsilon_0\epsilon_1}} \qquad \eta_2 = \sqrt{\frac{\mu_0}{\epsilon_0\epsilon_2}} \qquad (7)$$

ϵ_1 and ϵ_2 are the relative permittivities of air and water, respectively, while μ_0 and ϵ_0 are the permeability and permittivity of free space. ϵ_2 is a function of RF frequency and water salinity, and in this work we compute its value using the model developed by *Klein* and *Swift* [6].

Variation in ρ^{PP} with polarization and grazing angle are important factors in this multipath scattering model. This variation is illustrated in Figure 2 where the magnitude and phase of ρ^{PP} as computed from

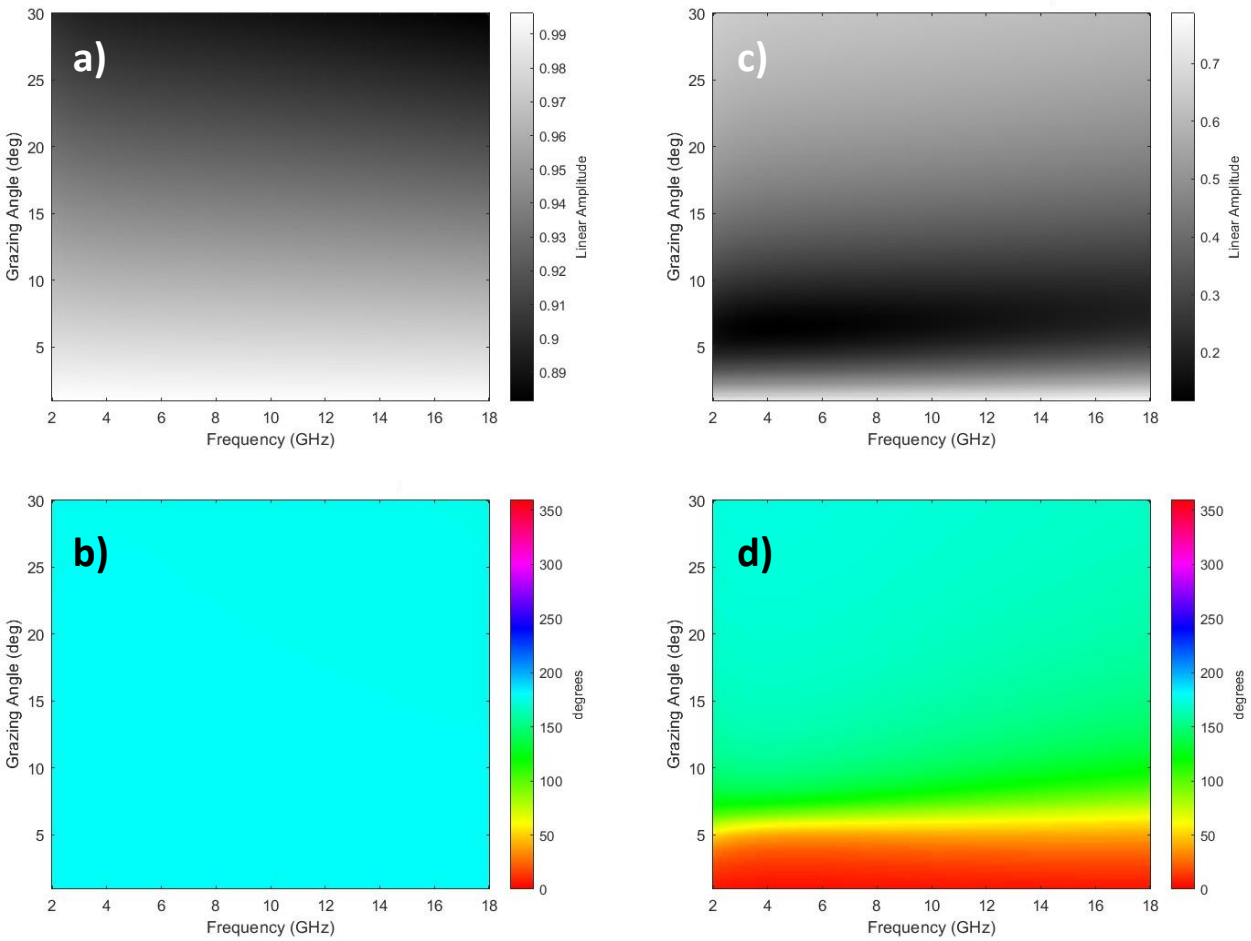

Figure 2. Magnitude and phase of the water reflection coefficient as a function of RF frequency and grazing angle, assuming a salinity of 32.53 ppt and a temperature of 20° C. **a)** HH magnitude **b)** HH phase **c)** VV magnitude **d)** VV phase

Eqns. 4-7 is plotted as a function of frequency and grazing angle. While the magnitude of ρ^{HH} is near 1 over the 0°-30° grazing angle range and its phase is nearly constant at 180° (i.e. $\rho^{HH} \cong -1$), both the magnitude and phase of ρ^{VV} vary significantly with grazing angle. The magnitude is largest for very small angles and falls to a minimum less than 0.2 in a band for 5° < ψ < 10°. The phase changes rapidly in this range as well, from a value near 0° for the lowest grazing angles up to approximately 180° for ψ=30°. This significant reduction in $|\rho^{VV}|$ for 5° < ψ < 10° is approximately described by the well-known Brewster angle phenomenon for reflection and transmission at an interface between two lossless dielectrics, in which energy with polarization in the plane of incidence (VV in the present case) is completely transmitted into the second medium for an angle, the Brewster angle, given by $\psi_B = \pi/2 - \tan^{-1}\sqrt{\epsilon_2/\epsilon_1}$. For the present case in which the second medium (water) is lossy and thus ϵ_2 is complex, the analysis is more complicated, but $|\rho^{VV}|$ still reaches a minimum near ψ_B.

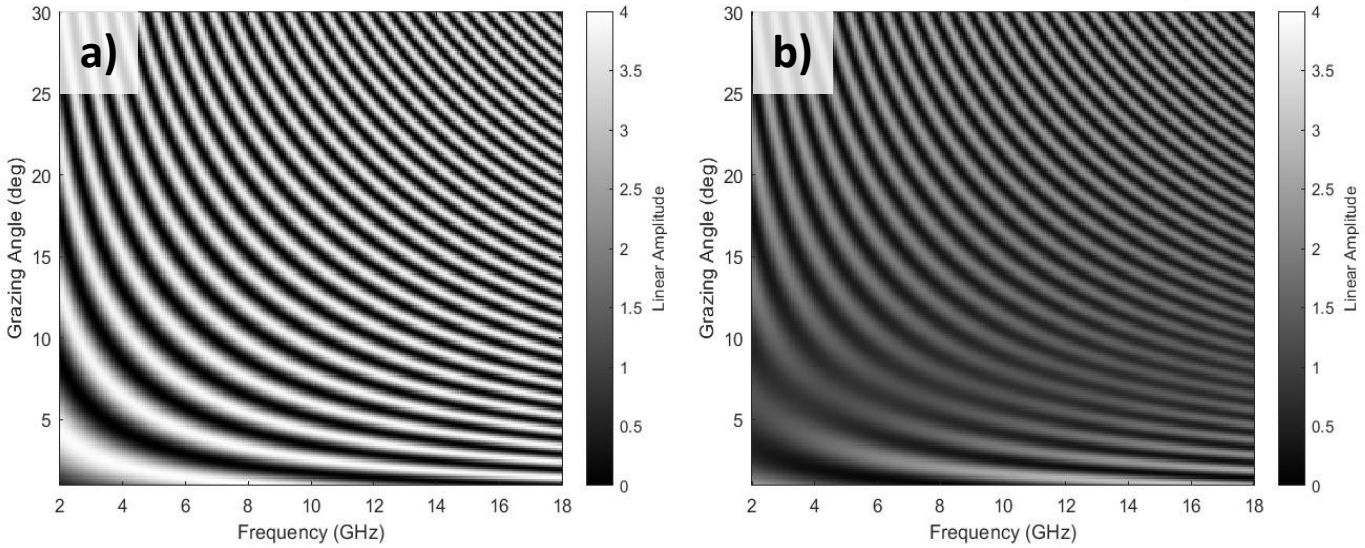

Figure 3. Backscatter magnitude (relative linear scale) for a breaker with a height h=0.5 m as a function of RF frequency and grazing angle **a)** HH **b)** VV

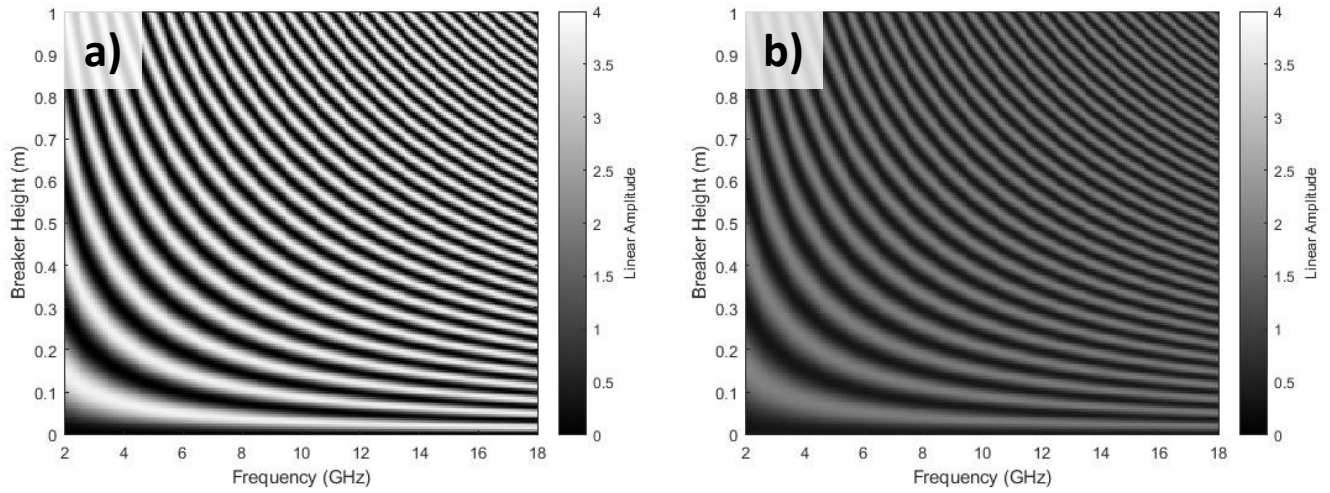

Figure 4. Backscatter magnitude (relative linear scale) for a breaker at a grazing angle $\psi = 15°$ as a function of RF frequency and breaker height **a)** HH **b)** VV

The behavior of the multipath model (Eqns. 2 and 3) for 0° < ψ < 30° and for a radar frequency, f, between 2 and 18 GHz is illustrated by Figures 3-6. For simplicity and a lack of knowledge to the contrary, it is assumed that $r_{pq}^{PP} = 1$ for all frequencies. Figure 3 shows the magnitude of the backscattered signal assuming a breaker height of 0.5 m. The interference fringes are obvious, and the figure also shows that the peak-to-null contrast of the fringes is greater for horizontal polarization than for vertical, a consequence of $|\rho^{HH}| > |\rho^{VV}|$. Additional reduction in the fringe contrast due to the Brewster angle is also evident for vertical polarization (Fig. 3b) in the range 5° < ψ < 10°. The behavior of the model as a function of frequency and breaker height at a grazing angle of ψ = 15° is shown in Figures

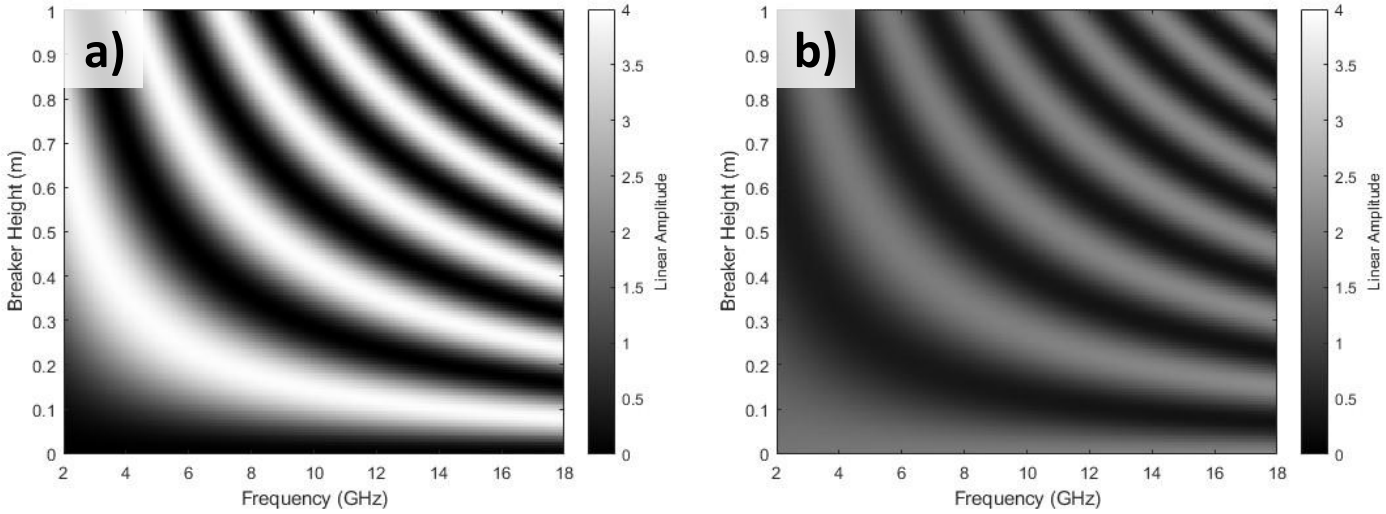

Figure 5. Backscatter magnitude (relative linear scale) for a breaker at a grazing angle $\psi = 3°$ as a function of RF frequency and breaker height **a)** HH **b)** VV

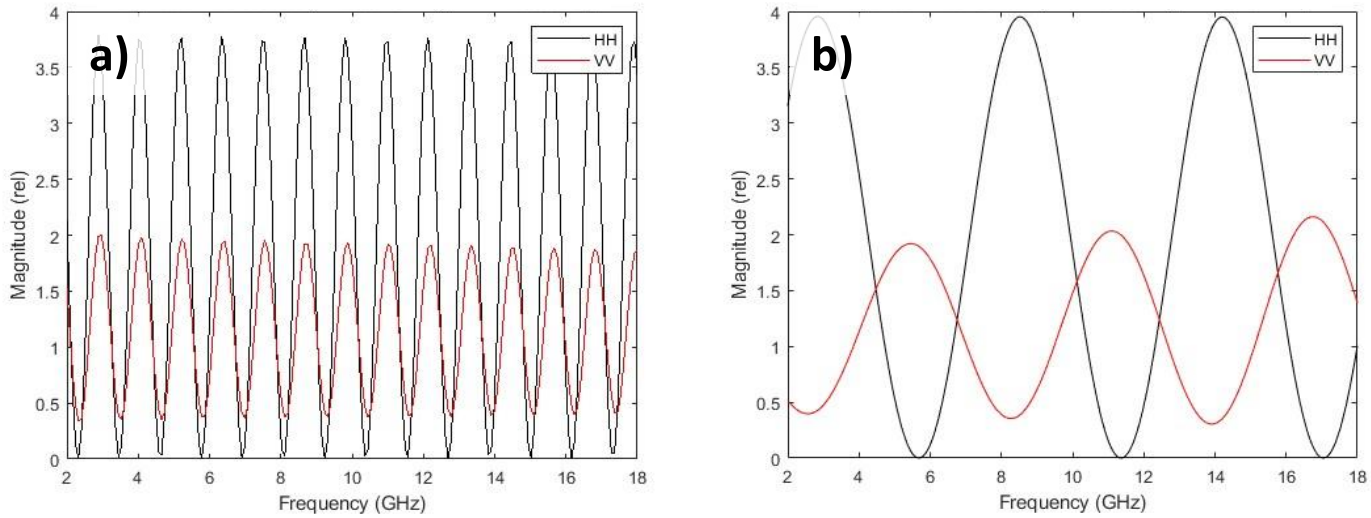

Figure 6. Backscatter magnitude (relative linear scale) for a breaker with height *h*=0.5 m as a function of RF frequency **a)** grazing angle $\psi = 15°$ **b)** grazing angle $\psi = 3°$

4a and 4b and for ψ= 3° in Figures 5a and 5b. The spacing between the fringes is seen to increase as the grazing angle decreases. This is highlighted in Figure 6 which display cuts across the previous figures at a breaker height of 0.5 m. Note that in 6b, the VV and HH responses are essentially complementary (i.e. minima in HH aligned with maxima in VV and vice versa), a result of the nearly 180° phase difference between ρ^{HH} and ρ^{VV} at very low grazing angles, as shown in Figures 2b and 2d. In Figure 6a, the VV and HH responses are essentially in phase.

Extraction of Breaker Height

As briefly outlined in [16], this multipath model can be used to estimate breaker height when applied to ultrawideband radar data. In this approach, we assume that the r_{pq}^{PP} factors are relatively constant (in both magnitude and phase) across the radar's RF bandwidth, and we exploit the known *insensitivity* of ρ^{PP} to frequency, as illustrated in Figure 2. The frequency response of the breaker is then determined by the simple exponential factors in Eqns. 2 and 3. In particular, the interference fringes seen in Figures 3-5 occur at frequencies f_1 and f_2 satisfying

$$k_2\Delta - k_1\Delta = \frac{2\pi}{c}(f_2 - f_1)\Delta = \mathrm{n}2\pi \qquad (8)$$

where c is the speed of light. Assuming n=1, i.e. considering two adjacent fringes, we obtain

$$\Delta = \frac{c}{f_2 - f_1} \qquad (9)$$

Combining this with Eqn. 1 produces the following expression for the breaker height

$$h = \frac{c}{2\sin(\psi)\,(f_2 - f_1)} \qquad (10)$$

Thus, if two adjacent fringes can be identified and the grazing angle is known, the breaker height can be estimated.

This analysis requires that the bandwidth, B, of the radar system be at least as wide as the frequency spacing between the two adjacent fringes. Setting this limit as $B = f_2 - f_1$ in Eqn. 9 leads to

$$B = \frac{c}{\Delta} \quad (11)$$

This is the absolute *minimum* bandwidth, corresponding to a fringe peak on each edge of the radar band. From a practical standpoint, the bandwidth should be approximately twice this value to allow detection and accurate location of the fringes in a more general case. The following inequality then describes the relationship between the required system bandwidth, grazing angle, and breaker height:

$$B \geq \frac{2c}{\Delta} = \frac{c}{h\sin(\psi)} \qquad (12)$$

This limit is plotted in Figure 7. As shown, the required bandwidth becomes quite large (relative to typical microwave radars) for the lowest grazing angles and/or small wave heights.

Figure 6 suggest two reasons why very low grazing angles are advantageous when using this approach to breaker height estimation. First, the wider fringe spacing produced by very low grazing angles (as in

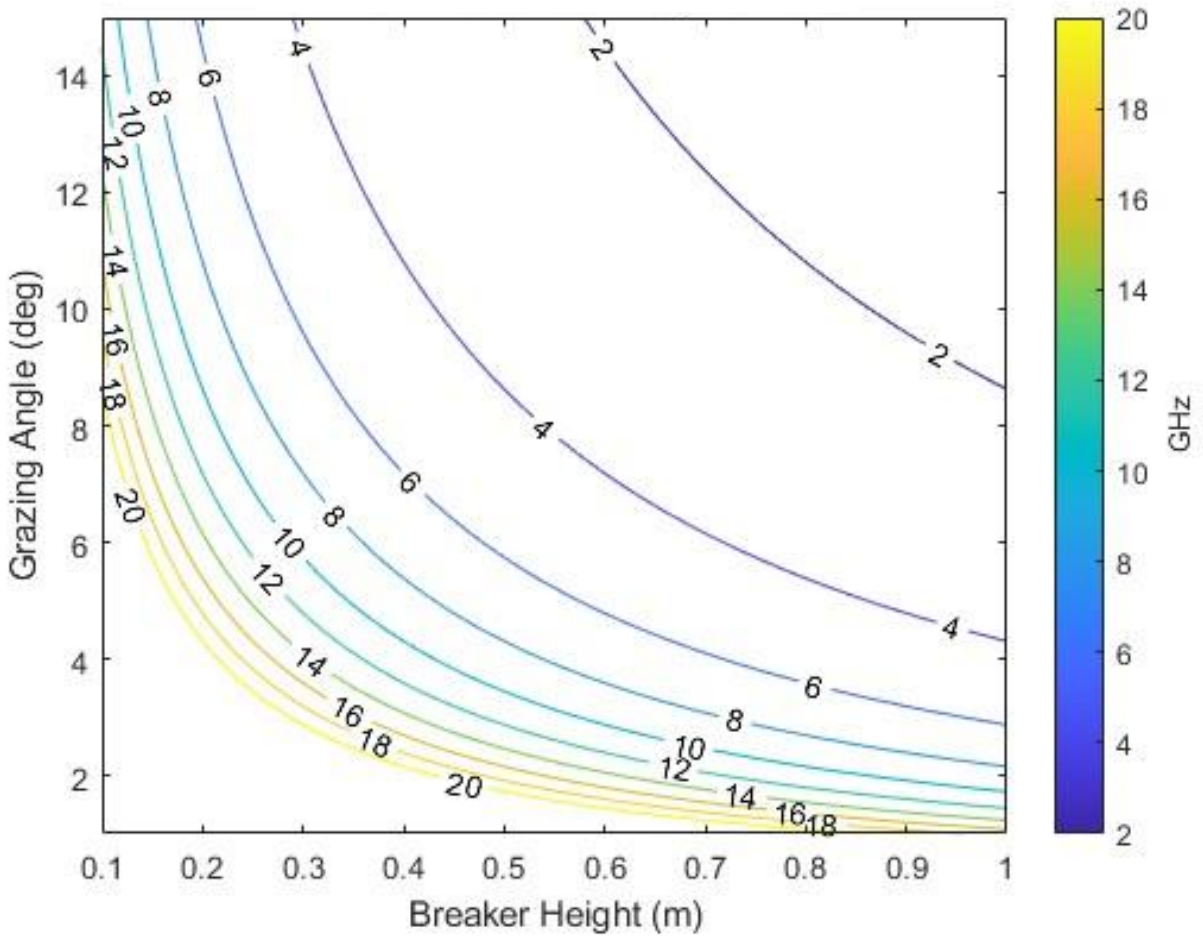

Figure 7. Minimum bandwidth requirement (GHz) as a function of breaker height and grazing angle

Figure 6b) means the fringes are easier to resolve. As discussed in more detail below, the intent is to apply Eqn. 10 to short segments of the entire, much longer range profile, with the length of the segments commensurate with the expected response of an isolated breaker. At ψ = 15°, it may be impossible to use such a short window while also producing the fine frequency resolution required to resolve the closely spaced fringes. (Note that frequency resolution is inversely proportional to the length of the time-domain window being analyzed.) Using a very low grazing angle relaxes the frequency resolution requirement. Second, the complementary character of the VV and HH responses seen for ψ= 3° can be used to identify those signals produced by the desired multipath scattering. Note that coherent interference between the signals produced by a localized group of individual scattering centers (as opposed to multipath from a single breaker) could also produce frequency domain fringes, and analysis of those signals using Eqn. 10 would obviously produce an erroneous estimate of breaker

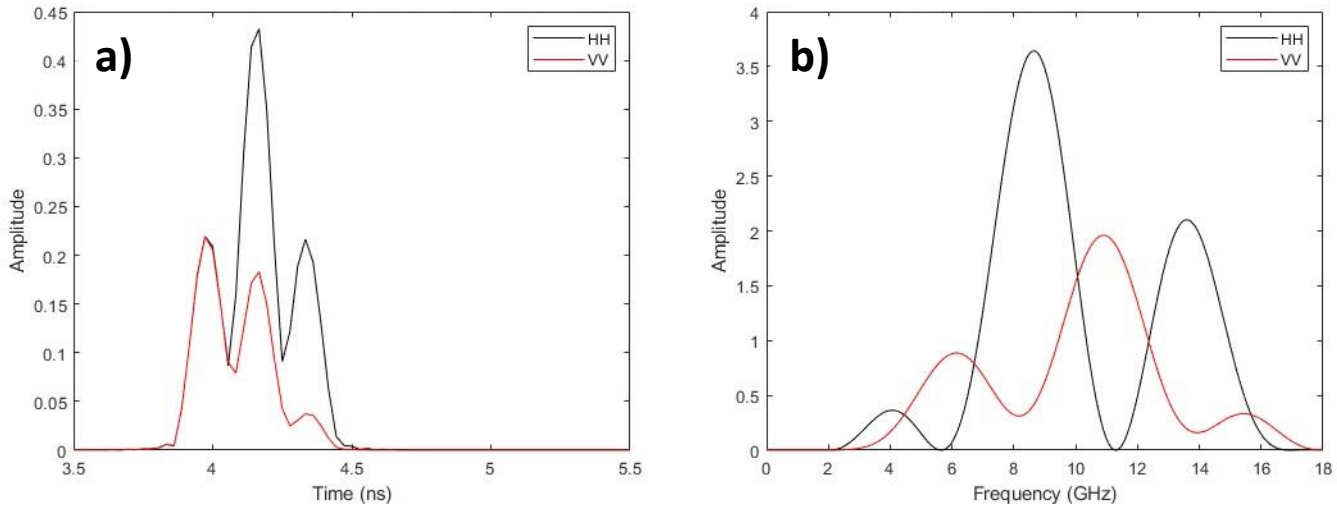

Figure 8. Backscatter magnitude (relative linear scale) for a breaker with height *h*=0.5 m at a grazing angle $\psi = 3°$ assuming a radar with a tapered 2-18 GHz bandwidth **a)** compressed profile in range/time domain **b)** RF frequency response

height. But the VV and HH responses of such a group are *not* expected to be complementary. By applying the method at very low grazing angles and by considering only those signals with a complementary polarization response, the distinctive phase of the front-face reflection coefficient ρ^{PP} can be exploited to reject these undesired signals.

Exploitation of the phase response of ρ^{PP} is also why a time-domain approach to breaker height estimation is expected to be less robust than the frequency domain analysis outlined in this paper. Given that the length of a radar pulse with bandwidth B is $\delta_r = c/B$, Eqns. 11 and 12 can be interpreted to mean that the algorithm can be applied so long as the range resolution is fine enough to spatially resolve the dd, di, and ii components of the multipath signal. Thus in a time-domain approach, Δ could be directly measured as the spacing between the range-resolved signals produced by these components. h could then computed from Eqn. 1. This is illustrated in Figure 8a where range-compressed backscatter produced by a 0.5 m breaker at ψ= 3°is displayed, assuming a 2-18 GHz radar with a Hanning (frequency domain) taper. The *dd*, *di*, and *ii* components are clearly visible as the three peaks in the range profile. However, as discussed in the previous paragraph, an independent group of three scattering centers can also produce a similar range profile. Thus a *time-domain* approach designed to estimate breaker height through detection and analysis of such signal patterns would be prone to error. But analysis of the *frequency domain* response of the same range-resolved signal, shown in Figure 8b, can provide increased robustness by indicating the presence of the complementary polarization response. With a better understanding of the actual values of the plume scattering coefficients, r_{pq}^{PP}, it

might be possible to develop a time-domain approach that rejects undesired signals based upon the relative strengths of the range-resolved dd, di, and ii components of the VV and HH signals. Differences in the relative strengths are in fact clearly evident in Figure 8a. But whether or not such a detailed model is representative of actual breaking wave backscatter is an open question. In contrast, the frequency domain approach outlined in this paper exploits only the lowest order features of the multipath scattering model and is therefore expected to be more robust.

The basic processing steps in this proposed height estimation approach are as follows. The analysis begins with the HH and VV range profiles. A short, sliding FFT window is first used to produce a time-frequency matrix for each polarization channel. The width of the FFT window should be selected to be commensurate with the estimated spatial/temporal extent of the breaker response. At each time step in the time-frequency matrix, a peak detection algorithm is applied to the frequency response, and Eqn. 10 then applied. To help evaluate the effects of noise or non-multipath scattering mechanisms (as discussed above), the height estimates should be binned by signal-to-noise ratio (SNR) as well as by some measure of the complementary character of the polarization response. An average height estimate could also be computed using the bin values as weighting factors.

References

[1] Dano, E. B., D. R. Lyzenga, and M. Perlin, Radar backscatter from mechanically generated transient breaking waves—part I: Angle of incidence dependence and high resolution surface morphology, *IEEE J. Oceanic Eng*., 26(2), 2001a.

[2] Dano, E. B., D. R. Lyzenga, G. Meadows, L. Meadows, H. V. Sumeren, and R. Onstott, Radar backscatter from mechanically generated transient breaking waves—part II: Azimuth and grazing angle dependence, *IEEE J. Oceanic Eng*., 26(2), 2001b.

[3] Ericson, E., D. R. Lyzenga, and D. T. Walker, Radar backscatter from stationary breaking waves, *J. Geophys. Res*., 104(C12), 29,679–29,695, 1999.

[4] Fuchs, J., and M. P. Tulin, Laboratory measurements of the joint dependence of radar frequency and water wavelength on sea spike returns, paper presented at *International Geoscience and Remote Sensing Symposium (IGARSS '98*), Inst. of Electr. and Electron. Eng., Seattle, Wash., 6–10 July 1998.

[5] Fuchs, J., D. Regas, T. Waseda, S. Welch, and M. Tulin,Correlation of hydrodynamic features with LGA radar backscatter from breaking waves, *IEEE Trans. Geosci. Remote Sens*., 37(5), 1999.

[6] Klein L. and C. Swift, An Improved Model for the Dielectric Constant of Sea Water at Microwave Frequencies, *IEEE Trans. Antennas Propag*., 25(1), 1977.

[7] Holliday, D., L. L. DeRaad, and G. J. St.-Cyr, Sea-spike backscatter from a steepening wave, *IEEE Trans. Antennas Propag*., 46(1), 1998.

[8] Ja, S.-J., J. C. West, H. Qiao, and J. H. Duncan, Mechanisms of low-grazing-angle scattering from spilling-breaker water waves, *Radio Sci.,* 36(5), 981–998, 2001.

[9] Kwoh, D. S., and B. M. Lake, A deterministic, coherent, and dual-polarized laboratory study of microwave backscattering from water waves, part I: Short gravity waves without wind, *IEEE J. Oceanic Eng*., 9(5), 1984.

[10] Lee, P. H. Y., J. D. Barter, K. L. Beach, C. L. Hindman, B. M. Lake, H. Rungaldier, H. R. Thompson, and R. Yee, Experiments on Bragg and non-Bragg scattering using single-frequency and chirped radars, *Radio Sci.*, 32(5), 1725–1744, 1997.

[11] Lee, P. H. Y., J. D. Barter, K. L. Beach, B. M. Lake, H. Rungaldier, H. R. Thompson, and R. Yee, Scattering from breaking gravity waves without wind, *IEEE Trans. Antennas Propag*., 46(1), 1998.

[12] Loewen, M. R., and W. K. Melville, Microwave backscatter and acoustic radiation from breaking waves, *J. Fluid Mech*., 224, 601–623, 1991.

[13] Plant, W. J., P. H. Dahl, and W. C. Keller, Microwave and acoustic scattering from parasitic capillary waves, *J. Geophys. Res*., 104(C11), 25,853–25,866, 1999b.

[14] Ramo S., J. Whinnery, and T. Van Duzer, *Fields and Waves in Communication Electronics*, John Wiley and Sons, 1965

[15] Sletten, M.A., J. West, X. Liu, and J. Duncan, "Radar Investigations of Breaking Water Waves at Low Grazing Angles with Simultaneous High-Speed Optical Imagery", *Radio Science*, Vol. 38, No. 6, December 2003.

[16] Sletten, M. A., Multipath scattering in ultrawide-band radar sea spikes, *IEEE Trans. Antennas Propag*., 46(1), 1998.

[17] Sletten, M. A., and J. Wu, Ultrawideband, polarimetric radar studies of breaking waves at low grazing angles, *Radio Sci.,* 31(1), 181–192, 1996.

[18] Sletten, M. A., D. B. Trizna, and J. P. Hansen, Ultrawideband radar observations of multipath propagation over the sea surface, *IEEE Trans. Antennas Propag*., 44(5), 1996.

[19] Trizna, D. B., J. P. Hansen, P. Hwang, and J. Wu, Laboratory studies of radar sea spikes at low grazing angles*, J. Geophys. Res*., 96(C7), 12,529–12,537, 1991.

[20] Walker, D. T., D. R. Lyzenga, E. A. Ericson, and D. E. Lund, Radar backscatter and surface roughness measurements for stationary breaking waves, *Proc. R. Soc. London*, Ser. A, 452, 1953–1984, 1996.

[21] West, J. C., Low-grazing-angle (LGA) sea-spike backscattering from plunging breaker crests, *IEEE Trans. Geosci. Remote Sens*., 40(2), 523–526, 2002.

[22] West, J. C., and S.-J. Ja, Two-scale treatment of low-grazing angle scattering from spilling breaker water waves, *Radio Sci*., 37(4), 1054, doi:10.1029/2001RS002517, 2002.

[23] West, J. C., and M. A. Sletten, Multipath EM scattering from breaking ocean waves at grazing incidence, *Radio Sci*., 32(4), 1455–1467, 1997.

[24] West, J. C., J. M. Sturm, and J.-S. Ja, Low-grazing scattering from breaking water waves using an impedance boundary MM/GTD approach, *IEEE Trans. Antennas Propag*., 46(1), 93–100, 1998.

[25] Zhao, Z., and J. C. West, Electromagnetic modeling of multipath scattering from breaking water waves with rough faces, *IEEE Trans. Geosci. Remote Sensing*, 2003.